Joint Reconfiguration of Feeders and Allocation of Capacitor Banks in Radial Distribution Systems Considering Voltage-Dependent Models

Juan M. Home-Ortiz, Renzo Vargas, Leonardo H. Macedo, Rubén Romero*

São Paulo State University, Avenida Brasil 56, Centro, 15385-000, Ilha Solteira, SP, Brazil

Abstract

This paper presents a study about operation planning for radial distribution systems using a mixed-integer second-order cone programming formulation. The proposal consists of a complete model for solving the problems of the reconfiguration of feeders and allocation of capacitor banks simultaneously, with the objective of achieving a minimum overall investment, in both fixed and switchable capacitor banks, and operational costs, related to the cost of energy losses. The approach includes a voltage-dependent load representation, as well as a precise representation of the operation of capacitor banks, which is also voltage dependent. The use of a mixed-integer second-order cone programming model guarantees convergence to optimality using existing optimization software. A strategy to reduce the number of candidate nodes of the system for capacitor banks allocation is also presented. Several tests are performed using the 69-node distribution system and a real 2313-node distribution system, demonstrating the effectiveness of the proposal. The results indicate that better solutions can be obtained by performing the simultaneous optimization of the reconfiguration and allocation of capacitor banks than by solving the two problems sequentially, which may even lead to infeasible solutions. It is also verified that both the load and capacitor banks models have an influence on the problem's solution.

Keywords: Allocation of capacitor banks; mixed-integer second-order cone programming; optimization; reconfiguration of distribution systems; voltage-dependent models.

Nomenclature

Sets:

Ω_ℓ	Set of load nodes;
Ω_s	Set of substation nodes;
Ω_B	Set of branches;
Ω_C	Set of capacitor module options;
Ω_{DG}	Set of nodes with distributed generation;
Ω_L	Set of load levels;
Ω_N	Set of nodes, $\Omega_N = \Omega_\ell \cup \Omega_s$.

Parameters:

b^C	Susceptance of a capacitor module;
c^C	Annualized cost of a capacitor module;
c_l^E	Price of the energy losses at load level l;
c^I	Annualized installation cost of a capacitor bank;
c^{SW}	Annualized cost of the switching equipment for a capacitor bank;
$\overline{n}_i^C$	Maximum number of capacitor modules at node i;
$\overline{I}_{ij}$	Maximum current magnitude of branch ij;

*Principal corresponding author

E-mail addresses: juanmanuelhome@gmail.com (Juan M. Home-Ortiz), rvargaspe@gmail.com (Renzo Vargas), leohfmp@ieee.org (Leonardo H. Macedo), ruben@dee.feis.unesp.br (Rubén Romero).

$\overline{N}^{C}$ Maximum number of capacitor banks in the system;

$\underline{pf}_{i}^{DG}$ Limit of the capacitive power factor of the distributed generator at node i;

$\overline{pf}_{i}^{DG}$ Limit of the inductive power factor of the distributed generator at node i;

$P_{i,l}^{o}$ Active power load at the nominal voltage magnitude V_o at node i at load level l;

$Q_{i,l}^{o}$ Reactive power load at the nominal voltage magnitude V_o at node i at load level l;

R_{ij} Resistance of branch ij;

$\overline{S}_{i}^{S}$ Maximum apparent power limit of a substation at node i;

$\underline{V}$ Minimum voltage magnitude;

$\overline{V}$ Maximum voltage magnitude;

V_o Nominal voltage magnitude;

X_{ij} Reactance of branch ij;

Z_{ij} Magnitude of the impedance of branch ij;

$\mathcal{Q}^{C}$ Nominal power of a capacitor module, at 1 p.u. voltage;

$\gamma_{i,l}^{I}$ Participation of constant current load on the active power demand at node i at load level l;

$\gamma_{i,l}^{P}$ Participation of constant power load on the active power demand at node i at load level l;

$\gamma_{i,l}^{Z}$ Participation of constant impedance load on the active power demand at node i at load level l;

$\phi_{i,l}^{I}$ Participation of constant current load on the reactive power demand at node i at load level l;

$\phi_{i,l}^{P}$ Participation of constant power load on the reactive power demand at node i at load level l;

$\phi_{i,l}^{Z}$ Participation of constant impedance load on the reactive power demand at node i at load level l;

Δ_l Duration of load level l.

Continuous Variables:

$I_{ij,l}^{sq}$ Square of the current magnitude of branch ij at load level l;

$P_{ij,l}$ Active power flow of branch ij at load level l;

$P_{i,l}^{DG}$ Active power generation by the distributed generator at node i at load level l;

$P_{i,l}^{S}$ Active power generation by the substation at node i at load level l;

$Q_{ij,l}$ Reactive power flow of branch ij at load level l;

$Q_{i,c,l}^{C}$ Reactive power injected at node i by the capacitor module c, at load level l;

$\hat{Q}_{i,l}^{C}$ Total reactive power injection by the capacitor bank at node i at load level l;

$Q_{i,l}^{DG}$ Reactive power generation by the distributed generator at node i at load level l;

$Q_{i,l}^{S}$ Reactive power generation by the substation at node i at load level l;

$V_{i,l}$ Voltage magnitude at node i at load level l;

$V_{i,l}^{sq}$ Square of the voltage magnitude at node i at load level l;

$\lambda_{ij,l}^{V}$ Slack variable used in the squared voltage drop magnitude calculation of branch ij at load level l;

$\lambda_{ij,l}^{\mathcal{V}}$ Slack variable used in the voltage drop magnitude calculation of branch ij at load level l;

β_{ij} Auxiliary variable used in the radiality constraints.

Integer Variables:

n_{i}^{C} Integer variable that indicates the number of capacitor modules installed at node i;

$\hat{n}_{i,l}^{C}$ Integer variable that represents the number of capacitor modules connected at node i at load level l;

q_{i}^{C} Binary variable that indicates whether a capacitor bank is installed at node i ($q_{i}^{C}=1$) or not ($q_{i}^{C}=0$);

q_{i}^{SW} Binary variable that indicates whether a switching equipment is installed with the capacitor bank at node i ($q_{i}^{SW}=1$) or not ($q_{i}^{SW}=0$);

$w_{i,c,l}^{C}$ Binary variable that indicates whether capacitor module c, of the capacitor bank at node i, is operating at load level l ($w_{i,c,l}^{C}=1$) or not ($w_{i,c,l}^{C}=0$);

y_{ij} Binary variable that indicates whether branch ij is connected to the system ($y_{ij}=1$) or not ($y_{ij}=0$).

1. Introduction

The need for improvements in power supply quality by electricity utilities has inspired several strategies, such as the allocation of capacitor banks and network reconfiguration in distribution systems [1], among others [2–4]. The installation of capacitor banks offers diverse benefits to the distribution network, e.g., improving the system's voltage profile, providing reactive power compensation, and reducing energy losses. The reconfiguration of distribution systems can be used to alleviate the feeders' loading, improve the voltage profile, and reduce losses by modifying the network topology.

In the specialized literature, several works have tackled the problem of the sizing and allocation of capacitor banks and the distribution feeders' reconfiguration problem separately. For the capacitor banks allocation, heuristic approaches can be found in [5,6]. Metaheuristic algorithms that try to avoid convergence to locally optimal solutions are proposed in [7–10], based on the tabu search, genetic, and particle swarm algorithms. A mathematical formulation to be solved by exact methods is proposed by [11], which presents a two-stage strategy, using a conic optimization model for the first stage, considering capacitor banks' sizes as continuous variables; then, mixed-integer linear programming is applied at the second stage, assuming the capacitor banks' sizes to be discrete variables. Although the capacitor allocation problem is widely addressed in the literature, the model for the reactive power injection by the capacitor banks to the distribution system is generally assumed to be constant, as the nominal rating, independent of the voltage at the node in which the bank is installed. For the distribution feeders' reconfiguration, several approaches, especially heuristic and metaheuristic techniques, have been developed, with different objectives. Heuristic algorithms to solve this problem can be found in [12,13]. On the other hand, metaheuristic techniques have also been used to solve the problem, such as simulated annealing in [14], the tabu search in [15], and the genetic algorithms in [16–18]. A multiobjective evolutionary algorithm is proposed in [19], in which the loads are represented through intervals to account for the uncertainties. In [20], a modified bacterial foraging algorithm is adapted to solve the reconfiguration problem of distribution systems. Mathematical models that can be solved using optimization solvers by exact techniques can also be used to solve the reconfiguration problem, as in [21,22]. A linearized formulation obtained from a mixed-integer nonlinear model in the presence of distributed generation is presented in [22]. In [21], a conic convex programming model is presented; the radiality is considered to be a set of spanning tree constraints. The authors in [23] use a spanning tree theory and propose a heuristic approach to solve the problem and show the impact on the power losses when voltage-dependent loads are incorporated in the reconfiguration problem.

The network reconfiguration and the capacitor banks allocation problems in radial distribution systems have been addressed simultaneously due to the shared objective functions, such as the minimization of power

losses and the necessity of maintaining the voltage system profile between adequate values in order to achieve an overall optimal solution. In [24], active power losses of the distribution network are minimized by alternately solving the capacitor banks allocation problem and the network reconfiguration problem with a genetic algorithm and a heuristic algorithm, respectively. The work of [25] presents a single dynamic data structure for evolutionary programming for simultaneous reconfiguration and capacitor banks allocation, to maximize system loadability. The authors of [26] use an efficient method for energy loss reduction based on the system state characterization performing reconfiguration after capacitor placement. In [27], both the reconfiguration and capacitor allocation are resolved through an ant colony search algorithm. The authors of [28] present a genetic algorithm strategy for solving the joint problem of reconfiguration and capacitor banks allocation. In [29], the reconfiguration and capacitor allocation problems are solved using a heuristic approach in order to minimize energy losses. The work of [30] presents a branch exchange method for solving the reconfiguration problem, while a genetic algorithm approach optimizes the size and location of capacitors within an integrated framework. In [31], a fuzzy binary gravitational search algorithm is used for improving system efficiency by solving the reconfiguration and the capacitor allocation problems. The authors introduce in [32] a new perturbation particle swarm optimization method for solving the reconfiguration and capacitor allocation problems simultaneously, by considering nonlinear loads. In [33], a krill herd algorithm is modified through opposition-based learning strategies for the optimal location of capacitor banks together with the reconfiguration problem. Finally, [34] presents a symbiotic organisms search in combination with a particle swarm optimization algorithm to improve the search space exploration for the capacitor placement and reconfiguration network problems. It can be verified that the joint problem of reconfiguration and capacitor banks allocation problems have been solved through heuristics- and metaheuristics-based strategies, whereas the voltage dependence of the capacitor's reactive power contribution to the network is, usually, disregarded.

In the literature, there are also works that solve the joint problem of the reconfiguration of feeders and operation of capacitor banks, assuming that the capacitor banks are already installed in the system [35]. In [36], a simulated annealing algorithm is used to solve the reconfiguration problem, while the capacitor operation is solved in a two-stage algorithm. The first stage finds the optimal continuous shunt susceptances that minimize the power losses, and then, in the second stage, and using the optimal continuous values, a Taylor approximation of losses is used to find the discrete values for the capacitor banks. In [37], the authors use an ant colony and harmony search to solve the network reconfiguration and capacitor banks switching problem in the presence of distributed generation, considering generation uncertainty. A two-step heuristic algorithm is proposed in [38]. In the first step, a binary particle swarm optimization algorithm is employed to determine a reduced set of feasible reconfigurations that are evaluated using a nonlinear optimal power flow (OPF); the objective function of this OPF minimizes the energy production cost. The second step determines the optimal switching of the already-installed capacitor banks

for each previously obtained reconfiguration, using exhaustive search. In [39], a two-stage robust reactive power optimization model is presented to coordinate discrete and continuous reactive power compensators, considering the power output uncertainty in installed wind farms.

Most of the papers present heuristic and metaheuristic approaches to solve the problem of feeders' reconfiguration and capacitor banks allocation, either considering only one of these problems or both problems simultaneously. Although heuristic-based methods are able to find good-quality solutions with low computational efforts, and metaheuristics are robust, flexible methods that can avoid the main drawback of heuristics, i.e., convergence to low-quality local optimal solutions, neither method can guarantee convergence to optimality [40]. Besides that, metaheuristics-based approaches present many issues, such as a high computational demand, the necessity of adjusting parameters, and the need to define a stop criterion.

Regarding the formulation of the problem, voltage-dependent models for capacitor banks and loads are disregarded in the clear majority of works [2]. This fact may provide solutions that can be not only suboptimal for the more precise model, with voltage-dependent loads and capacitor banks operations, but also infeasible and costly with respect to the investment, as was verified in the tests presented.

In this work, a complete mathematical model for the problem of the simultaneous reconfiguration of feeders and allocation of capacitor banks is presented. The proposed approach considers investment in both fixed and switchable capacitor banks and aims to minimize the overall investment and operational costs. The proposed formulation includes voltage-dependent loads by using the polynomial model presented in [41]. Besides that, the reactive power injection of the capacitor banks is formulated using an accurate model that considers reactive power injections as a function of the voltage magnitude in which the bank is installed. The resulting model is a mixed-integer second-order cone programming problem, which is convex; therefore, optimality can be achieved by using existing optimization software. A new strategy to reduce the number of candidate nodes for capacitor banks allocation is also presented.

The main contributions and conclusions of this paper are the following:

i. A new convex complete formulation, of mixed-integer second-order cone programming, for the simultaneous reconfiguration of feeders and capacitor banks allocation, which ensures convergence to the optimal solution of the problem;
ii. Voltage-dependent models considered for the representation of the operation of the capacitor banks and loads. This type of representation, which is more precise than constant power models, is widely neglected in existing works that optimize either the reconfiguration problem or the capacitor banks allocation problem;

iii. A new, efficient strategy to reduce the number of candidate nodes for installing capacitor banks in large distribution systems. The results indicate that the proposed strategy is capable of defining candidate nodes without excluding the optimal solution of the problem;

iv. The results show that it is important to perform the joint optimization of the feeders' reconfiguration and capacitor banks allocation, since solving the two problems sequentially may lead to suboptimal or even infeasible solutions, as presented in the results for the first system;

v. The influence of the model used to represent the operation of the capacitor banks and the loads is also analyzed—it was demonstrated that when the optimization of the considered problem is performed using the constant power models, commonly used in the literature, the obtained results are infeasible for the voltage-dependent formulation, which is a more realistic representation of the real-world problem.

The remainder of this paper is organized as follows: Section 2 presents the proposed formulation for the problem; Section 3 presents a strategy to reduce the number of candidate nodes for installing capacitor banks in large systems; Section 4 presents the results for several tests performed with the 69-node test system and a 2313-node real system; Section 5 presents a discussion about the obtained results; and Section 6 presents the conclusions of the work.

2. Mathematical Formulation

This section presents the mixed-integer second-order cone programming model for the problem of joint reconfiguration of feeders and capacitor banks allocation in distribution systems considering voltage-dependent loads. The proposed model provides a solution with both optimal investment in fixed and switchable capacitor banks, with their location and number of modules at the system's nodes, as well as the optimal operation of the switchable banks for each load level. A single optimal topology is obtained simultaneously by reconfiguration to operate at all load levels.

2.1 Objective Function

The objective function v shown in (1) considers both the investment cost in capacitor banks and the operational costs.

$$\min v = \sum_{i \in \Omega_\ell} (c^I q_i^C + c^{SW} q_i^{SW} + c^C n_i^C) + \sum_{l \in \Omega_L} \sum_{ij \in \Omega_B} c_l^E \Delta_l R_{ij} I_{ij,l}^{sq} \tag{1}$$

Capacitor banks can be installed at load nodes, and in the first sum of (1), the first term, $c^I q_i^C$, is related to the installation cost of a capacitor bank at a node. Therefore if $q_i^C = 1$, then a capacitor bank is installed at node

i, and the installation cost c^I is added to the objective function, independently of the number of modules of the bank. The second term, $c^{SW}q_i^{SW}$, is related to the purchase and installation costs of the switching devices for capacitor banks. If $q_i^{SW}=1$, then the capacitor bank installed at node i is switchable, and the cost, c^{SW}, is added to the objective function. The third term, $c^C n_i^C$, is related to the cost of purchasing the capacitor modules, c^C, according to the number of capacitor modules added to the bank at node i, n_i^C. Note that all of the investment costs are annualized, and the parameter Δ_l represents the number of hours of operation for load level l, considering an operation period of one year. The second part of the objective function represents the cost of energy losses in the system for a one-year horizon.

2.2 Network Operation Modeling

The operation of the network is represented by the power flow equations presented in (2)–(8), based on the branch-flow formulation presented in [42].

$$\sum_{ki\in\Omega_B} P_{ki,l} - \sum_{ij\in\Omega_B}\left(P_{ij,l}+R_{ij}I^{sq}_{ij,l}\right)+P^S_{i,l}+P^{DG}_{i,l}=\left(\gamma^Z_{i,l}\frac{V^{sq}_{i,l}}{V_o^2}+\gamma^I_{i,l}\frac{V_{i,l}}{V_o}+\gamma^P_{i,l}\right)P^o_{i,l} \quad \forall i\in\Omega_N, l\in\Omega_L \quad (2)$$

$$\sum_{ki\in\Omega_B} Q_{ki,l} - \sum_{ij\in\Omega_B}\left(Q_{ij,l}+X_{ij}I^{sq}_{ij,l}\right)+Q^S_{i,l}+Q^{DG}_{i,l}+\hat{Q}^C_{i,l} = \left(\phi^Z_{i,l}\frac{V^{sq}_{i,l}}{V_o^2}+\phi^I_{i,l}\frac{V_{i,l}}{V_o}+\phi^P_{i,l}\right)Q^o_{i,l} \quad \forall i\in\Omega_N, l\in\Omega_L \quad (3)$$

$$V^{sq}_{i,l}-V^{sq}_{j,l}+\lambda^V_{ij,l}=2(R_{ij}P_{ij,l}+X_{ij}Q_{ij,l})+Z^2_{ij}I^{sq}_{ij,l} \quad \forall ij\in\Omega_B, l\in\Omega_L \quad (4)$$

$$V^{sq}_{j,l}I^{sq}_{ij,l}\geq P^2_{ij,l}+Q^2_{ij,l} \quad \forall ij\in\Omega_B, l\in\Omega_L \quad (5)$$

$$\left|\lambda^V_{ij,l}\right|\leq\left(\overline{V}^2-\underline{V}^2\right)(1-y_{ij}) \quad \forall ij\in\Omega_B, l\in\Omega_L \quad (6)$$

$$V_{i,l}-V_{j,l}+\lambda^{\mathcal{V}}_{ij,l}=R_{ij}P_{ij,l}+X_{ij}Q_{ij,l} \quad \forall ij\in\Omega_B, l\in\Omega_L \quad (7)$$

$$\left|\lambda^{\mathcal{V}}_{ij,l}\right|\leq(\overline{V}-\underline{V})(1-y_{ij}) \quad \forall ij\in\Omega_B, l\in\Omega_L \quad (8)$$

Constraints (2) and (3) represent the active and reactive power balance in the system (Kirchhoff's current law), while (4) and (5) impose Kirchhoff's voltage law on the system operation, in all load levels. The slack variable, $\lambda^V_{ij,l}$, is calculated in (6) according to the status of the switch of branch ij, at load level l. That is, if $y_{ij}=1$ (the switch of branch ij is closed, and the branch is connected to the system), then $\lambda^V_{ij,l}=0$ and the difference $V^{sq}_{i,l}-V^{sq}_{j,l}$ is calculated in (4); otherwise, if $y_{ij}=0$ (the switch of branch ij is open, and the branch is not operating), then constraint (4) is not applied to the branch ij, and $V^{sq}_{i,l}$ and $V^{sq}_{j,l}$ are independent.

Constraints (2) and (3) use the polynomial load model, also known as the ZIP model, to represent the voltage dependency characteristic of loads. In this representation, the loads consist of constant impedance (Z),

constant current (I), and constant power (P) components, and the dependence of the voltage magnitude changes according to the participation, γ and ϕ, of each component. The value of each component can be in the interval [0,1] in the "constrained ZIP model" [41], or it can be greater than 1 and/or less than 0 in the "accurate ZIP model" [41]. However, the sum of the load participation, $\gamma^Z_{i,l} + \gamma^I_{i,l} + \gamma^P_{i,l}$ and $\phi^Z_{i,l} + \phi^I_{i,l} + \phi^P_{i,l}$, of each component at each node and each load level, must be equal to one [41]. For the constant power load model, $\gamma^P_{i,l} = \phi^P_{i,l} = 1$, and $\gamma^Z_{i,l} = \gamma^I_{i,l} = \phi^Z_{i,l} = \phi^I_{i,l} = 0$, while for voltage-dependent loads, many utilities consider $\gamma^Z_{i,l} = \gamma^I_{i,l} = 0.5$, $\gamma^P_{i,l} = 0$, $\phi^Z_{i,l} = 1$, and $\phi^I_{i,l} = \phi^P_{i,l} = 0$ [41].

The conditions for which the conic constraint (5) is active are presented in [42,43]. After solving the model, it must be verified if (5) is active for all branches and load levels considered.

Since the load is voltage-dependent, the terms related to the constant power and constant impedance (dependent of the square of the voltage magnitude, $V^{sq}_{i,l}$) in (2) and (3) are readily available. However, the constant current component is dependent of the voltage magnitude, which can be obtained by $\sqrt{V^{sq}_{i,l}}$. This would make the model nonlinear. To avoid this issue, the voltage magnitude drop is calculated in (7), which provides a good approximation for the voltages (tests have shown errors lower than 0.4%). The slack variable, $\lambda^{\mathcal{V}}_{ij,l}$, calculated in (8), is used to include constraint (7) in the model ($\lambda^{\mathcal{V}}_{ij,l} = 0$) or not ($\lambda^{\mathcal{V}}_{ij,l} = 1$), according to the status of the switch y_{ij} of branch ij.

Besides that, in the model, the voltages $V^{sq}_{i,l}$ and $V_{i,l}$ are fixed at the voltage magnitude value at the substation i, $\forall i \in \Omega_s, l \in \Omega_L$; $P^S_{i,l} = 0$; $Q^S_{i,l} = 0$ $\forall i \in \Omega_\ell, l \in \Omega_L$; and $Z_{ij} = \sqrt{R^2_{ij} + X^2_{ij}}$ $\forall ij \in \Omega_B$. For a branch ij without a switch, y_{ij} can be fixed at 1.

2.3 Physical and Operational Limits

The physical and operational limits for the system are represented in (9)–(14). Constraints (9) and (10) are the voltage limits in the system for the squared voltage magnitude and for the voltage magnitude, respectively.

$$\underline{V}^2 \leq V^{sq}_{i,l} \leq \overline{V}^2 \qquad \forall i \in \Omega_\ell, l \in \Omega_L \qquad (9)$$

$$\underline{V} \leq V_{i,l} \leq \overline{V} \qquad \forall i \in \Omega_\ell, l \in \Omega_L \qquad (10)$$

Constraint (11) represents the current limit of each branch ij, according to the status of the corresponding switch y_{ij}. Constraints (12) and (13) limit the active and reactive power flow on each branch ij and each load level l, according to y_{ij}.

$$0 \leq I_{ij,l}^{sq} \leq \overline{I}_{ij}^{2} y_{ij} \qquad \forall ij \in \Omega_B, l \in \Omega_L \qquad (11)$$

$$\left|P_{ij,l}\right| \leq \overline{VI}_{ij} y_{ij} \qquad \forall ij \in \Omega_B, l \in \Omega_L \qquad (12)$$

$$\left|Q_{ij,l}\right| \leq \overline{VI}_{ij} y_{ij} \qquad \forall ij \in \Omega_B, l \in \Omega_L \qquad (13)$$

The capacities of the substations are represented by the quadratic constraint (14).

$$(P_{i,l}^{S})^2 + (Q_{i,l}^{S})^2 \leq \left(\overline{S}_i^{S}\right)^2 \qquad \forall i \in \Omega_s, l \in \Omega_L \qquad (14)$$

The distributed generation limits are represented in (15)–(17).

$$(P_{i,l}^{DG})^2 + (Q_{i,l}^{DG})^2 \leq \left(\overline{S}_i^{DG}\right)^2 \qquad \forall i \in \Omega_{DG}, l \in \Omega_L \qquad (15)$$

$$P_{i,l}^{DG} \geq 0 \qquad \forall i \in \Omega_{DG}, l \in \Omega_L \qquad (16)$$

$$-P_{i,l}^{DG} \tan(\cos^{-1}(\underline{pf}_i^{DG})) \leq Q_{i,l}^{DG} \leq P_{i,l}^{DG} \tan\left(\cos^{-1}\left(\overline{pf}_i^{DG}\right)\right) \qquad \forall i \in \Omega_{DG}, l \in \Omega_L \qquad (17)$$

Constraints (15) and (16) represent the generation limits of the distributed generators installed in the system. Constraint (17) is the limit for the reactive power generation by the distributed generators. The presented limits must be satisfied at all load levels.

2.4 Radiality Constraints

The radiality of the network is imposed by (18)–(21), as proposed in [21], using spanning tree constraints.

$$\beta_{ij} + \beta_{ji} = y_{ij} \qquad \forall ij \in \Omega_B \qquad (18)$$

$$\beta_{ij} = 0 \qquad \forall ij \in \Omega_B | i \in \Omega_s \qquad (19)$$

$$\beta_{ji} = 0 \qquad \forall ij \in \Omega_B | j \in \Omega_s \qquad (20)$$

$$\sum_{j \in \Omega_N | ij \in \Omega_B \text{ or } ji \in \Omega_B} \beta_{ij} = 1 \qquad \forall i \in \Omega_\ell \qquad (21)$$

The status of the switch at branch ij is represented by y_{ij}, such that if $y_{ij} = 1$, then branch ij is connected to the system, and it is disconnected otherwise. Two auxiliary binary variables, β_{ij} and β_{ji}, are defined for each branch ij, indicating the direction of the flow in the branch, and constraint (18) imposes that only one direction is possible for a flow on branch ij if $y_{ij} = 1$, and if $y_{ij} = 0$, then both auxiliary variables are equal to 0 for branch ij. If the flow is from node j toward node i, then $\beta_{ij} = 1$, and $\beta_{ji} = 1$ if the flow is from i toward j. Constraints (19) and (20) impose that the flows can only leave the substation, i.e., for a branch ij in which node i is a substation node, then (19) imposes that $\beta_{ij} = 0$, indicating that $\beta_{ji} = 1$ (if $y_{ij} = 1$) and the flow must be from node i toward

node j. Constraint (20) is similar to (19), but refers to the branches in which node j is a substation node. Finally, constraint (21) imposes that, for each load node i, there is only one flow arriving, and all other flows must be leaving the node.

2.5 Investment and Operational Constraints for Capacitor Banks

This section presents two sets of constraints related to the investment and operation of capacitor banks. The first one is a simplified model that considers constant reactive power injection by the capacitor banks and is the most used formulation in works that solve the capacitor banks allocation problem, while the second one is a precise formulation, with voltage-dependent reactive power injection.

2.5.1 Capacitor Banks with Constant Reactive Power Injection Model

The first set of constraints is (22)–(26), which considers that the reactive power injection by a capacitor bank is independent of the voltage at the node in which the bank is installed, as considered in most works presented in the literature.

$$\hat{Q}^C_{i,l} = \hat{n}^C_{i,l} \mathcal{Q}^C \qquad \forall i \in \Omega_\ell, l \in \Omega_L \tag{22}$$

$$\hat{n}^C_{i,l} \leq n^C_i \qquad \forall i \in \Omega_\ell, l \in \Omega_L \tag{23}$$

$$n^C_i \leq \overline{n}^C_i q^C_i \qquad \forall i \in \Omega_\ell \tag{24}$$

$$\left|\hat{n}^C_{i,l} - \hat{n}^C_{i,l-1}\right| \leq \overline{n}^C_i q^{SW}_i \qquad \forall i \in \Omega_\ell, l \in \Omega_L | l > 1 \tag{25}$$

$$\sum_{i \in \Omega_\ell} q^C_i \leq \overline{N}^C \tag{26}$$

Constraint (22) defines $\hat{Q}^C_{i,l}$, the reactive power injection at node i at load level l, as the number of capacitor modules connected to node i at load level l, $\hat{n}^C_{i,l}$, multiplied by the nominal reactive power of a capacitor module, $\mathcal{Q}^C$. Note that in this model, the total injection, $\hat{Q}^C_{i,l}$, does not depend on the voltage at node i at load level l.

Constraint (23) limits the number of capacitor banks that are connected to node i at load level l, $\hat{n}^C_{i,l}$, to the number of capacitor modules installed at node i, n^C_i. In other words, for a capacitor module to be connected to a node, it must be installed at that node, and its price must be considered in the objective function.

Constraint (24) is used to indicate whether a capacitor bank is installed at node i or not. If $n^C_i > 0$, then $q^C_i = 1$, and the installation cost of the capacitor bank at node i is added to the investment cost. This constraint is also used to limit the number of capacitor banks installed at node i to a maximum of $\overline{n}^C_i$.

Constraint (25) indicates whether the capacitor bank installed at node i is switchable or not. If $q_i^{SW} = 0$, then $\left|\hat{n}_{i,l}^C - \hat{n}_{i,l-1}^C\right| = 0$, indicating that the number of capacitor banks connected to node i cannot change from one load level to another, which represents a fixed capacitor bank. Note that, in this case, the cost of the switching device is not added to the objective function. On the other hand, if $q_i^{SW} = 1$, the cost of the switching device is added to the investment cost, indicating that, at node i, there is a switchable capacitor bank, and in this case, $\left|\hat{n}_{i,l}^C - \hat{n}_{i,l-1}^C\right| \leq \overline{n}_i^C$, i.e., the number of capacitor modules connected to the system at consecutive load levels can vary from zero to the maximum number of capacitor modules installed at node i, as presented in constraint (23).

Finally, constraint (26) limits the number of nodes in the system in which capacitor banks can be installed to the value of $\overline{N}^C$.

2.5.2 Capacitor Banks with Voltage-Dependent Reactive Power Injection Model

A more realistic representation for the operation of the capacitor banks is proposed in constraints (27)–(34), in which the reactive power injection by a capacitor bank at a node is dependent on the voltage at that node.

$$\hat{Q}_{i,l}^C = \sum_{c \in \Omega_C} Q_{i,c,l}^C \qquad \forall i \in \Omega_\ell, l \in \Omega_L \tag{27}$$

$$-\overline{V}^2 b^C (1 - w_{i,c,l}^C) \leq Q_{i,c,l}^C - b^C V_{i,l}^{sq} \leq -\underline{V}^2 b^C (1 - w_{i,c,l}^C) \qquad \forall i \in \Omega_\ell, c \in \Omega_C, l \in \Omega_L \tag{28}$$

$$\underline{V}^2 b^C w_{i,c,l}^C \leq Q_{i,c,l}^C \leq \overline{V}^2 b^C w_{i,c,l}^C \qquad \forall i \in \Omega_\ell, c \in \Omega_C, l \in \Omega_L \tag{29}$$

$$w_{i,c,l}^C \leq w_{i,c-1,l}^C \qquad \forall i \in \Omega_\ell, c \in \Omega_C, l \in \Omega_L | c > 1 \tag{30}$$

$$\sum_{c \in \Omega_C} w_{i,c,l}^C \leq n_i^C \qquad \forall i \in \Omega_\ell, l \in \Omega_L \tag{31}$$

$$n_i^C \leq \overline{n}_i^C q_i^C \qquad \forall i \in \Omega_\ell \tag{32}$$

$$\left| \sum_{c \in \Omega_C} w_{i,c,l}^C - \sum_{c \in \Omega_C} w_{i,c,l-1}^C \right| \leq \overline{n}_i^C q_i^{SW} \qquad \forall i \in \Omega_\ell, l \in \Omega_L | l > 1 \tag{33}$$

$$\sum_{i \in \Omega_\ell} q_i^C \leq \overline{N}^C \tag{34}$$

In this formulation, a binary variable, $w_{i,c,l}^C$, is used to indicate whether the capacitor module c is connected to node i at load level l ($w_{i,c,l}^C = 1$) or not ($w_{i,c,l}^C = 0$). Therefore, the set of capacitor modules of a capacitor bank is represented by Ω_C, where each module is represented by an index c. The variable, $Q_{i,c,l}^C$, represents the reactive power injection at node i, by the capacitor module c, at load level l. Figure 1 is used to illustrate these considerations.

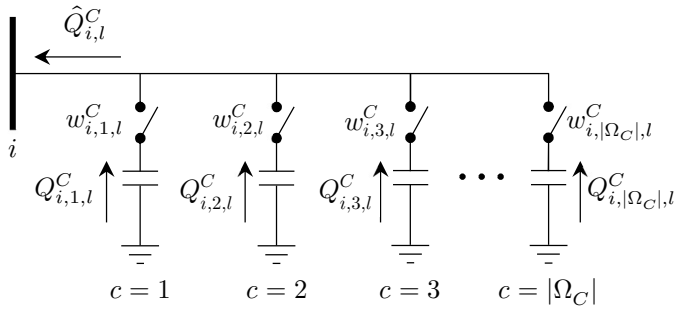

Figure 1: Capacitor bank model

Based on the proposed approach, constraint (27) defines the total reactive power injection by the capacitor bank at node i at load level l as the sum of injections of each capacitor module c, $Q^C_{i,c,l}$.

Constraints (28) and (29) represent a disjunctive formulation that calculates the reactive power injection of each individual capacitor module c, at node i at load level l, as a function of the voltage magnitude and the susceptance of the module, b^C. Note that if $w^C_{i,c,l} = 0$, then in (29), $Q^C_{i,c,l} = 0$, and in (28), $\underline{V}^2 \leq V^{sq}_{i,l} \leq \overline{V}^2$. On the other hand, if $w^C_{i,c,l} = 1$, then in (29), $Q^C_{i,c,l}$ must be within the minimum and maximum limits of the reactive power injection, which depend on the susceptance of the module and the minimum and maximum voltage magnitude limits in the system, and by (28), $Q^C_{i,c,l} = b^C V^{sq}_{i,l}$. Note that, if the limits for the voltage magnitude in the system are $\underline{V} = 0.95$ p.u. and $\overline{V} = 1.05$ p.u., then errors of up to 10.25% can appear in the reactive power injection of a capacitor bank if the first model, which does not consider voltage dependency, is used.

Equation (30) is a fencing constraint, which imposes that the capacitor module c, with $c > 1$, can only be connected to the system if the module $c - 1$ is already connected. Note that, if a capacitor bank has, for example, three modules, and two of them should be connected, then it makes no difference which one of them should be disconnected, since all of them have the same specification. This type of constraint does not modify the optimal solution of the problem, but it can help the efficiency of the solver for the problem.

Note that, in this second formulation for the capacitor banks' investment and operation, $\hat{n}^C_{i,l} = \sum_{c \in \Omega_C} w^C_{i,c,l}$, and therefore, constraints (31)–(33) are equivalent to (23)–(25). Constraint (34) remains the same as (26).

2.6 Operation and Investment Binary Variables

The discrete nature of some operation and investment variables is represented in (35)–(40).

$$q^C_i \in \{0,1\} \qquad \forall i \in \Omega_\ell \qquad (35)$$

$$q^{SW}_i \in \{0,1\} \qquad \forall i \in \Omega_\ell \qquad (36)$$

$$\beta_{ij}, \beta_{ji} \in \{0,1\} \qquad \forall ij \in \Omega_B, ji \in \Omega_B \qquad (37)$$

$$\hat{n}^C_{i,l} \in \mathbb{Z}^{\geq} \qquad \forall i \in \Omega_\ell, l \in \Omega_L \qquad (38)$$

$$w^{C}_{i,c,l} \in \{0,1\} \qquad \forall i \in \Omega_{\ell}, c \in \Omega_{C}, l \in \Omega_{L} \quad (39)$$

$$n^{C}_{i} \in \mathbb{Z}^{\geq} \qquad \forall i \in \Omega_{\ell} \quad (40)$$

Equation (35) defines the variable that indicates the presence of a capacitor bank at a node as a binary variable, while (36) defines the binary variable related to the installation of the switching device of a capacitor bank at a node. Equation (37) indicates the binary nature of the variable related to the switches of the branches, used to open or close a circuit. The operation of a capacitor bank is defined in the simplified model by the nonnegative integer variable, $\hat{n}^{C}_{i,l}$, presented in (38), and in the more precise model by the set of binary variables, $w^{C}_{i,c,l}$, presented in (39). Finally, the nonnegative integer variable, n^{C}_{i}, which indicates the number of capacitor modules installed at node i, is defined in (40).

2.7 Complete Models

Two different models can be obtained for the discussed problem. Both consider the simultaneous reconfiguration of feeders and allocation of capacitor banks with voltage-dependent loads.

In the first model (M1), however, the operation of the capacitor banks is simplified, and their reactive power injection is independent of the voltage magnitudes at the nodes in which they are installed. The model M1 is, therefore, formed by objective function (1), subject to (2)–(26) and (35)–(40).

The second model (M2) considers a precise representation of the operation of the capacitor banks, with voltage-dependent reactive power injections. The model M2 is formed by objective function (1), subject to (2)–(21), and (27)–(40).

Both models can also be solved considering only constant power demands, as is done in most works available in the literature, by fixing $\gamma^{Z}_{i,l}$, $\gamma^{I}_{i,l}$, $\phi^{Z}_{i,l}$, and $\phi^{I}_{i,l}$ at zero and $\gamma^{P}_{i,l}$ and $\phi^{P}_{i,l}$ at one, $\forall i \in \Omega_{N}, l \in \Omega_{L}$. Besides that, a solution for the reconfiguration problem alone can be obtained by fixing the investment variables related to the capacitor banks at zero and performing the reconfiguration. Similarly, a solution for the capacitor banks allocation alone can be obtained by fixing the topology of the network and solving the capacitor allocation problem.

Since the proposed models are convex, optimality can be ensured by solvers that use exact optimization techniques. The next section presents the results of several tests performed with the proposed models, considering a case available in the literature.

3. Strategy to Reduce the Number of Candidate Nodes for Capacitor Banks' Installation

The current generation of computational hardware and commercial optimization solvers may not be able to find a good-quality solution for the proposed formulation when large systems are considered. To deal with this

issue, a strategy to reduce the number of candidate nodes for capacitor banks' allocation, and consequently, to reduce the combinatorial search space of the problem, is presented in Figure 2.

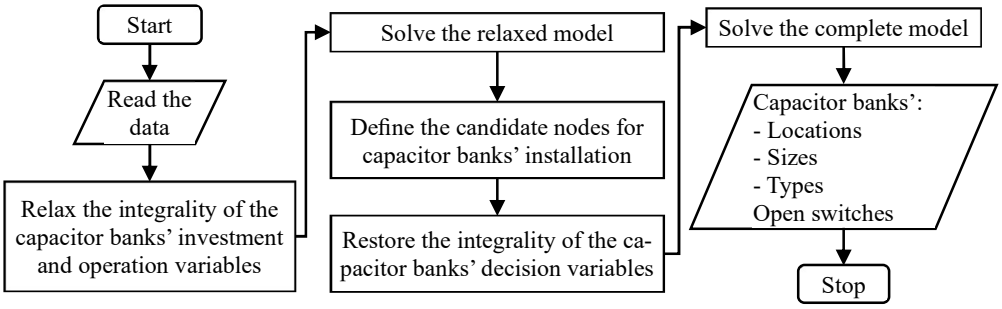

Figure 2: Flowchart for defining candidate nodes for installing capacitor banks

The proposed strategy for reducing the number of candidate nodes for capacitor banks installation begins with the system's data reading. Then, the integrality of the variables related to the capacitor banks installation, q_i^C, q_i^{SW}, and n_i^C, and the operation, $\hat{n}_{i,l}^C$ or $w_{i,c,l}^C$, is relaxed, i.e., constraints (35), (36), and (39) are replaced by $0 \leq q_i^C \leq 1$, $0 \leq q_i^{SW} \leq 1$, and $0 \leq w_{i,c,l}^C \leq 1$, respectively, and (38) and (40) are replaced by $\hat{n}_{i,l}^C \geq 0$ and $n_i^C \geq 0$, respectively. After that, the corresponding model is solved, considering only the binary variables of the reconfiguration problem. With the obtained solution, the candidate nodes are defined using the values of $\hat{Q}_{i,l}^C$, i.e., the nodes i with $\hat{Q}_{i,l}^C$ greater than $\underline{Q}^*$ for some l are defined as candidate nodes for the installation of capacitor banks.

After the candidate nodes are defined, the complete optimization model for the problem is solved with the discrete variables that correspond to the investment and operation of capacitor banks related to the nodes that are not candidates to receive a capacitor bank fixed at zero. The model will provide the final topology of the network, as well as the capacitor banks' sizes, locations, and types.

Ideally, this type of reduction should maintain in the candidate set of nodes, the nodes that would have capacitor banks installed if the complete model was solved, without the reduction. This is verified for the proposed strategy in the next section. It should be noted that the proposed reduction strategy can be used with all of the problem formulations presented.

4. Tests and Results

The proposed convex models for the reconfiguration of distribution systems and the allocation of capacitor banks, simultaneously considering voltage-dependent loads and capacitor banks operation, was implemented in AMPL [44] and solved with CPLEX version 12.8 [45] (with default settings and an optimality gap of 1%) on a computer with a 3.20 GHz Intel® Core™ i7-8700 CPU and 16 GB of RAM.

4.1 69-Node System

The 69-node system, adapted from [6,8,46], is used to test the proposed method. The voltage magnitude limits for the system are $\underline{V} = 0.95$ p.u. and $\overline{V} = 1.05$ p.u. Three load levels, 1-heavy, 2-medium, and 3-light, are considered, with durations $\Delta_1 = 1000$ h, $\Delta_2 = 6760$ h, and $\Delta_3 = 1000$ h [6], and the price of the energy losses $c_l^E = 0.06$ USD/kWh $\forall l \in \Omega_L$. The data for the capacitor banks are $c^I = 1000$ USD, $c^{SW} = 300$ USD, $c^C = 900$ USD [6], $\mathcal{Q}^C = 300$ kVAr, $\overline{n}_i^C = 6$ $\forall i \in \Omega_\ell$, and $\overline{N}^C = 6$. The initial configuration of the system, i.e., before the reconfiguration and allocation of the capacitor banks, is illustrated in Figure 3. The system has 68 load nodes, one substation node, and 73 lines. The nominal voltage of the system is 12.66 kV, and the capacity of the substation is 30 MVA. It is assumed that, for medium and light loads, the voltage at the substation is at 1 p.u., while, for heavy loads, the voltage is at 1.05 p.u. The complete data for this system are available in [47].

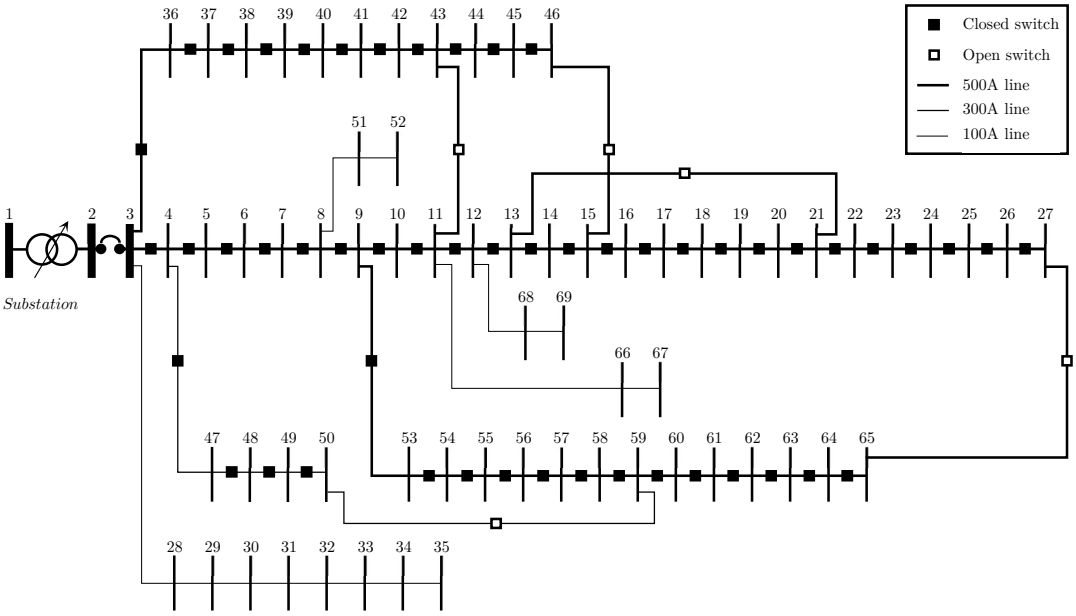

Figure 3: Initial configuration for the 69-node system

The following tests were considered:

Case A1: Simultaneous reconfiguration of feeders and allocation of capacitor banks, considering both constant power loads and nominal reactive power injection by the capacitor banks (model M1 with $\gamma_{i,l}^Z = 0$, $\gamma_{i,l}^I = 0$, $\gamma_{i,l}^P = 1$, $\phi_{i,l}^Z = 0$, $\phi_{i,l}^I = 0$, and $\phi_{i,l}^P = 1$ $\forall i \in \Omega_N, l \in \Omega_L$ [41]);

Case A2: Simultaneous reconfiguration of feeders and allocation of capacitor banks, considering constant power loads and voltage-dependent reactive power injection by the capacitor banks (model M2 with $\gamma_{i,l}^Z = 0$, $\gamma_{i,l}^I = 0$, $\gamma_{i,l}^P = 1$, $\phi_{i,l}^Z = 0$, $\phi_{i,l}^I = 0$, and $\phi_{i,l}^P = 1$ $\forall i \in \Omega_N, l \in \Omega_L$ [41]);

Case A3: Simultaneous reconfiguration of feeders and allocation of capacitor banks, considering voltage-dependent loads ($\gamma_{i,l}^Z = 0.5$, $\gamma_{i,l}^I = 0.5$, $\gamma_{i,l}^P = 0$, $\phi_{i,l}^Z = 1$, $\phi_{i,l}^I = 0$, and $\phi_{i,l}^P = 0$ $\forall i \in \Omega_N, l \in \Omega_L$ [41]) and nominal reactive power injection by the capacitor banks (model M1);

Case A4: Simultaneous reconfiguration of feeders and allocation of capacitor banks, considering both voltage-dependent loads ($\gamma^Z_{i,l} = 0.5$, $\gamma^I_{i,l} = 0.5$, $\gamma^P_{i,l} = 0$, $\phi^Z_{i,l} = 1$, $\phi^I_{i,l} = 0$, and $\phi^P_{i,l} = 0$ $\forall i \in \Omega_N, l \in \Omega_L$ [41]) and voltage-dependent reactive power injection by the capacitor banks (model M2).

Tables 1 and 2 present the results for Cases A1 and A2, which consider the constant load model and capacitor banks with nominal and voltage-dependent reactive power injections, respectively.

Table 1: Values of decision variables for Cases A1 and A2, which consider constant power demands

Results	Initial configuration	Cases											
		A1						A2					
Open switches	11-43, 13-21, 15-46, 50-59, 27-65	5-6, 13-14, 57-58, 63-64, 13-21						5-6, 13-14, 54-55, 63-64, 13-21					
Capacitor banks' location/ operation	–	Node	Modules	Type	Modules connected (reactive power injected [kVAr])			Node	Modules	Type	Modules connected (reactive power injected [kVAr])		
					Level 1	Level 2	Level 3				Level 1	Level 2	Level 3
		6	2	Fixed	2(600)	2(600)	2(600)	6	2	Fixed	2(552.55)	2(552.47)	2(576.81)
		11	3	Fixed	3(900)	3(900)	3(900)	11	3	Fixed	3(863.66)	3(845.94)	3(875.29)
		50	3	Fixed	3(900)	3(900)	3(900)	50	3	Fixed	3(949.18)	3(884.44)	3(894.53)
		59	3	Switchable	3(900)	0(0)	0(0)	59	4	Switchable	4(1141.54)	1(279.48)	1(228.45)
		61	6	Switchable	6(1800)	5(1500)	3(900)	61	6	Switchable	6(1633.63)	5(1365.16)	3(852.25)
		65	4	Switchable	4(1200)	2(600)	1(300)	64	4	Switchable	4(1087.82)	2(543.17)	1(282.80)

Table 2: Operational results for Cases A1 and A2

Results	Initial configuration	Cases	
		A1	A2
Investment cost (USD)	–	25,800.00	26,700.00
Total losses cost (USD)	403,449.90	148,643.38	148,737.27
Total cost (USD)	403,449.90	174,443.38	175,437.27
Node - Min. voltage (p.u.)			
Load level 1	65 - 0.7468	64 - 0.9516	64 - 0.9521
Load level 2	65 - 0.8525	64 - 0.9518	64 - 0.9515
Load level 3	65 - 0.9070	63 - 0.9691	64 - 0.9709
Power losses (kW)			
Load level 1	2449.58	794.58	798.92
Load level 2	596.89	233.57	233.20
Load level 3	239.62	103.87	103.58
Losses cost reduction (%)	–	63.16	63.13
CPU time (s)	–	242	584

Table 1 shows that, in the initial state of the system, the switches at branches 11-43, 13-21, 15-46, 50-59, and 27-65 are open, and the system does not have any capacitor bank. In this case, in Table 2, the losses cost is 403,449.90 USD, with minimum voltage magnitudes of 0.7468 p.u., 0.8525 p.u., and 0.9070 p.u. at node 65 for the load levels 1–3, respectively.

For Case A1, with the reconfiguration opening the switches of branches 5-6, 13-14, 57-58, 63-64, and 13-21 and closing all other switches, and with the capacitor banks allocated at six nodes, with a total investment cost of 25,800.00 USD (and their operation described in the table), the losses cost was reduced by 63.16%, to 148,643.38 USD, and all the voltage magnitudes are, in this case, within the limits of 0.95 p.u. and 1.05 p.u.

In Case A2, which considers the reactive power injection by the capacitor banks represented by the voltage-dependent model, a similar reduction in the cost of losses in the system, of 63.13%, was obtained, when compared to Case A1. In this case, however, the topology of the system is different, with the switches of branches 5-6, 13-14, 54-55, 63-64, and 13-21 open. Also, the investment in capacitor banks is larger (26,700.00 USD), the banks are installed at different nodes, and their operation differs from Case A1. It can be verified in the operation of the capacitor banks in Case A2 that the reactive power injections differ from the nominal values. For example, at node 6, at load level 1, two modules, with a nominal reactive power $\mathcal{Q}^C = 300$ kVAr each, are injecting 552.55 kVAr, representing a difference of 8.59% from the nominal value. It is worth noting that the solution for Case A1 is infeasible when it is fixed in Case A2, due to the voltage magnitude violation at the nodes and current limits violation, since the capacitor banks cannot provide enough reactive power compensation to the system.

Tables 3 and 4 present the results for Cases A3 and A4, which consider the voltage-dependent load model and the capacitor banks with nominal and voltage-dependent reactive power injections, respectively.

Table 3: Values of decision variables for Cases A3 and A4, which consider voltage-dependent loads

Results	Initial configuration	Cases											
		A3						A4					
Open switches	11-43, 13-21, 15-46, 50-59, 27-65	5-6, 13-14, 57-58, 61-62, 13-21						5-6, 14-15, 56-57, 61-62, 13-21					
Capacitor banks' location/ operation	–	Node	Modules	Type	Modules connected (reactive power injected [kVAr])			Node	Modules	Type	Modules connected (reactive power injected [kVAr])		
					Level 1	Level 2	Level 3				Level 1	Level 2	Level 3
		6	2	Fixed	2(600)	2(600)	2(600)	6	2	Fixed	2(552.05)	2(550.96)	2(572.61)
		11	2	Fixed	2(600)	2(600)	2(600)	11	2	Fixed	2(574.25)	2(561.87)	2(579.21)
		49	6	Switchable	6(1800)	3(900)	2(600)	49	6	Switchable	6(1913.89)	3(886.21)	2(593.35)
		61	6	Switchable	6(1800)	4(1200)	3(900)	61	6	Switchable	6(1626.92)	5(1371.67)	3(844.87)
		65	4	Switchable	4(1200)	2(600)	1(300)	64	4	Switchable	4(1085.84)	2(541.95)	1(280.84)

Table 4: Operational results for Cases A3 and A4

Results	Initial configuration	Cases	
		A3	A4
Investment cost (USD)	–	23,900.00	23,900.00
Total losses cost (USD)	253,173.16	133,326.39	133,694.25
Total cost (USD)	253,173.16	157,226.39	157,594.25
Node - Min. voltage (p.u.)			
Load level 1	65 - 0.8346	62 - 0.9506	62 - 0.9506
Load level 2	65 - 0.8802	62 - 0.9506	62 - 0.9501
Load level 3	65 - 0.9185	62 - 0.9673	62 - 0.9673
Power losses (kW)			
Load level 1	1306.94	725.61	731.79
Load level 2	403.23	207.41	207.49
Load level 3	186.77	94.43	93.84
Losses cost reduction (%)	–	47.34	47.19
CPU time (s)	–	550	391

In the base case, considering voltage-dependent loads, the losses cost is 253,173.16 USD. The minimum voltage in the system at all load levels are under the minimum limit of 0.95 p.u., but the minimum voltages are

higher than those of the base case with constant power loads. Also, the losses in the system are lower when this model is considered.

The results for Cases A3 and A4 indicate the same investment cost (23,900.00 USD), with different topologies for the network and different locations and operations for the capacitor banks. The reductions in the cost of the losses were almost the same in both cases. After the reconfiguration, the operation of the system becomes feasible, with all the voltages within the range of 0.95 p.u. and 1.05 p.u. Note again that the solutions for Cases A3 and A4 differ from the solutions for Cases A1 and A2, both in the topology of the network and the investment and operation of the capacitor banks.

Figure 4 shows the voltage profile in the system for Cases A1–A4, compared to the base case. Figure 4 (a)–(d) indicates that the voltage profile is improved in the system in all four cases, and the operation of the system becomes feasible with respect to the voltage magnitude constraint.

To show the importance of considering voltage-dependent models for the loads and the operation of the capacitor banks, Tables 5 and 6 present the results obtained when the binary variables that represent the network topology for the reconfiguration problem and the discrete variables that represent the capacitor banks investment and operation of Cases A1–A3 are fixed in Case A4, i.e., the integer solutions for Cases A1–A3 are analyzed using the complete voltage-dependent formulation.

By analyzing Tables 5 and 6, it can be verified that the solutions for Cases A1 and A2 present both higher investment and losses costs when they are evaluated with the considerations of Case A4. Besides that, although the voltage magnitude constraint is satisfied by both solutions, the current magnitude constraint is violated in branch 3-4, at load level 1, and therefore, both solutions are infeasible. It was only possible to obtain them by increasing the current capacity of the branches. The integer variables of the solution for Case A3 are infeasible when they are fixed in the model of Case A4 because the minimum voltage magnitude in the system is lower than 0.95 p.u.

The importance of performing the simultaneous reconfiguration of feeders and allocation of capacitor banks is evidenced when these problems are solved sequentially. In both cases, for the test system presented, considering both constant power and voltage-dependent loads, it is not possible to obtain a feasible solution by solving either the reconfiguration and then the allocation or the allocation and then the reconfiguration problem.

It should be noted that the conic constraint (5) was active on all branches, at all load levels, and in all test cases. Finally, the computational times for Cases A1–A4 were 242 s, 584 s, 550 s, and 391 s, respectively. This indicates that the approach can be applied to larger instances.

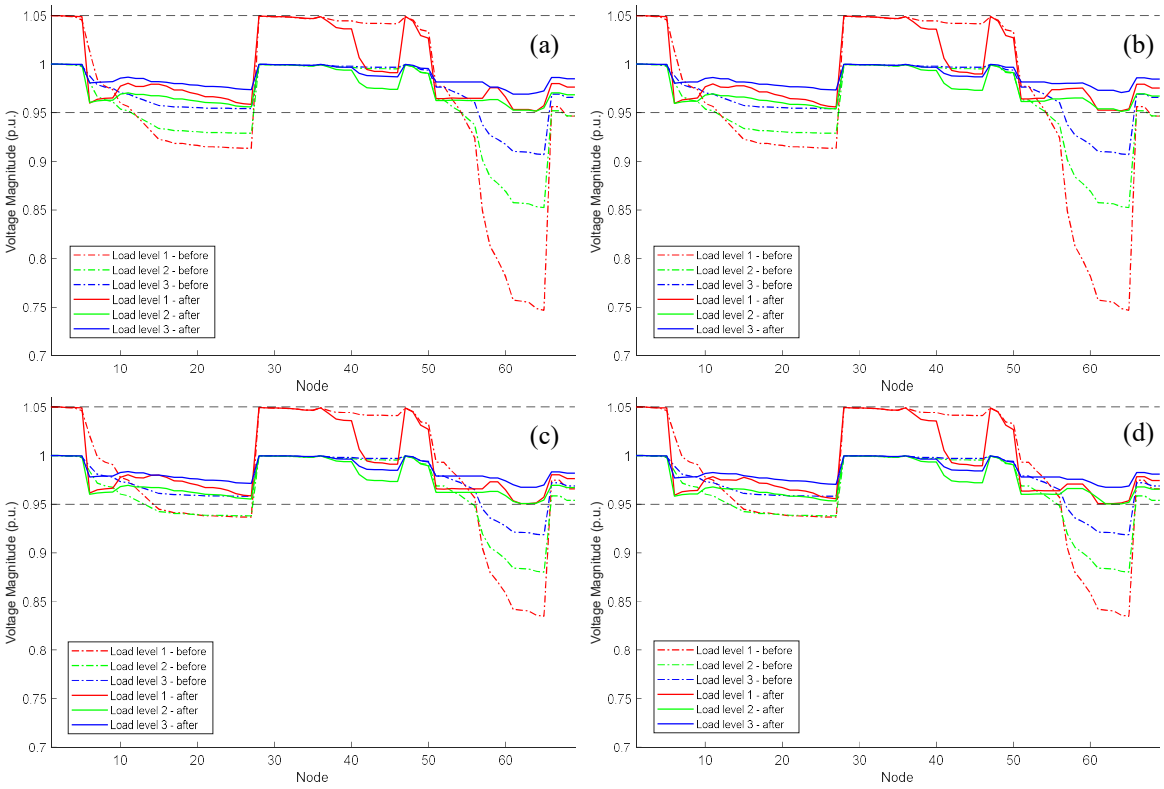

Figure 4: Voltage profile in the 69-node system for (a) Case A1, (b) Case A2, (c) Case A3, and (d) Case A4

Table 5: Values of decision variables for Cases A1, A2, and A3 fixed in the complete model of Case A4

Results	Cases											
	A1				A2				A3			
Open switches	5-6, 13-14, 57-58, 63-64, 13-21				5-6, 13-14, 54-55, 63-64, 13-21				5-6, 13-14, 57-58, 61-62, 13-21			
Capacitor banks' location/ operation	Node	Modules connected (reactive power injected [kVAr])			Node	Modules connected (reactive power injected [kVAr])			Node	Modules connected (reactive power injected [kVAr])		
		Level 1	Level 2	Level 3		Level1	Level 2	Level 3		Level 1	Level 2	Level 3
	6	2(557.82)	2(556.07)	2(577.64)	6	2(559.73)	2(557.17)	2(578.42)	6	2(552.32)	2(551.07)	2(572.67)
	11	3(870.30)	3(850.57)	3(876.44)	11	3(872.35)	3(851.77)	3(877.30)	11	2(574.53)	2(561.97)	2(579.28)
	50	3(949.93)	3(884.24)	3(892.30)	50	3(952.42)	3(887.21)	3(895.57)	49	6(1913.90)	3(883.44)	2(593.35)
	59	3(864.30)	0(0)	0(0)	59	4(1160.35)	1(282.39)	1(289.58)	61	6(1626.92)	4(1083.90)	3(844.87)
	61	6(1656.11)	5(1369.94)	3(847.79)	61	6(1667.65)	5(1382.48)	3(856.31)	65	4(1091.82)	2(543.61)	1(281.56)
	65	4(1109.95)	2(550.06)	1(284.35)	64	4(1107.33)	2(549.33)	1(283.95)				

Table 6: Operational results for Cases A1, A2, and A3 fixed in the complete model of Case A4

Results	Cases		
	A1	A2	A3
Investment cost (USD)	25,800.00	26,700.00	23,900.00
Total losses cost (USD)	133,089.08	134,380.23	133,547.67
Total cost (USD)	158,889.08	161,080.23	157,447.67
Node - Min. voltage (p.u.)			
Load level 1	64 - 0.9564	64 - 0.9606	62 - 0.9471
Load level 2	64 - 0.9545	64 - 0.9568	62 - 0.9482
Load level 3	63 - 0.9705	64 - 0.9729	62 - 0.9663
Power losses (kW)			
Load level 1	718.57	722.16	729.56
Load level 2	207.50	209.93	207.44
Load level 3	96.89	98.38	93.97
Losses cost reduction (%)	47.43	46.92	47.25

An additional test was carried out to evaluate the possibility of solving the exact mixed-integer nonlinear programming problem obtained when constraint (5) is replaced by an equality, $V_{i,l}^{sq}$ is replaced by $V_{i,l}^{2}$, and constraints (7)–(9) are removed from the model. The optimization solver KNITRO was used in this test, and it was not able to obtain a feasible integer solution for the problem. This result indicates that mixed-integer nonlinear programing problems are still a challenge to overcome, even for medium-sized systems.

4.2 Validation of the Strategy to Reduce the Number of Candidate Nodes for Capacitor Banks Allocation

Ideally, the reduction strategy should provide a set of candidate nodes for the installation of capacitor banks that does not exclude the optimal solution of the problem, i.e., a node at which a capacitor bank is installed when the model is solved without the reduction should be a candidate node.

Since the optimal solution is only known after the complete model is solved, and very large systems may be difficult to solve with the current generation of optimization solvers and computational hardware, to evaluate the effectiveness of the reduction strategy, a test was carried out using the 69-node system.

By applying the reduction strategy to the 69-node system with $\underline{Q}^{*} = 0$, the set of candidate nodes for the installation of capacitor banks, Ω_{ℓ}^{*}, is $\Omega_{\ell}^{*} = \{6, 11, 12, 49, 50, 59, 61, 64, 65\}$. It can be verified that the solutions for Cases A1–A4, obtained without the reduction strategy, have capacitor banks installed only at the candidate nodes obtained with the reduction strategy. This indicates that the proposed reduction strategy did not exclude the optimal solution of the problem.

4.3 2313-Node Real System

In order to validate the scalability of the proposed formulations for large instances, results for a real system based on a Colombian oil company are presented. This system operates at 14.4 kV and is composed of 2305 load nodes, 2335 branches, six substations of 15 MVA, and two distributed generation nodes, each one with a capacity of 10 MVA. The total active and reactive loads are 59.579 MW and 28.855 MVAr, respectively. The strategy to reduce the number of candidate nodes was applied to the system, and in this case, for $\underline{Q}^{*} = 0$, 140 nodes are classified as candidates for the installation of capacitor banks. Complete data for this system can be found in [47]. Two cases are considered:

Case B1: Simultaneous reconfiguration of feeders and allocation of capacitor banks, considering both constant power loads and nominal reactive power injection by the capacitor banks (model M1);

Case B2: Simultaneous reconfiguration of feeders and allocation of capacitor banks, considering both voltage-dependent loads and voltage-dependent reactive power injection by the capacitor banks (model M2).

Table 7 presents the initial operating state of the system, considering both constant power and voltage-

dependent models for the loads. It can be verified that the operation is infeasible in both cases because the minimum voltage magnitude in the system is under the minimum limit of 0.95 p.u.

Table 7: Initial state of the system

Results	Constant power load model	Voltage-dependent load model
Open switches	110-122, 175-139, 225-346, 250-1301, 366-272, 594-619, 646-602, 799-800, 815-816, 816-793, 919-853, 939-933, 961-946, 989-1052, 969-1045, 962-966, 1079-1136, 1261-2297, 1284-1185, 1299-586, 1300-349, 1303-396, 186-71, 655-572, 332-1296, 725-606, 1307-615	
Total losses cost (USD)	889,188.31	863,011.67
Total generation cost (USD)	492,299.22	473,054.21
Total cost (USD)	1,381,487.53	1,336,065.89
Node - Min. voltage (p.u.)		
Load level 1	1890 - 0.8541	1890 - 0.8630
Load level 2	1890 - 0.8875	1890 - 0.8928
Power losses (kW)		
Load level 1	2107.47	2038.82
Load level 2	1276.05	1245.09

Tables 8 and 9 present the results for Cases B1, B2, and the operation obtained when the integer solution for Case B1 is fixed in the complete voltage-dependent model.

Table 8: Values of decision variables for Cases B1 and B2

Results	Cases														
	B1					B2					Case B1 fixed in the complete model				
Open switches	1301-1279, 192-961, 393-1046, 658-802, 505-2297, 650-741, 940-2297, 149-146, 646-816, 1308-644, 110-122, 225-346, 366-272, 746-1853, 799-800, 919-853, 989-1052, 962-966, 1079-1136, 1261-2297, 1284-1185, 1299-586, 1300-349, 1303-396, 186-71, 655-572, 725-606, 1307-615					1301-1279, 192- 961, 658- 802, 505-2297, 650- 741, 940-2297, 149-146, 646- 816, 1308- 644, 110 -122, 225 -346, 366 -272, 746-1853, 799- 800, 919- 853, 989-1052, 969-1045, 962- 966, 1079-1136, 1261-2297, 1284-1185, 1299- 586, 1300- 349, 1303- 396, 186-71, 655-572, 725- 606, 1307- 615					1301-1279, 192-961, 393-1046, 658-802, 505-2297, 650-741, 940-2297, 149-146, 646-816, 1308-644, 110-122, 225-346, 366-272, 746-1853, 799-800, 919-853, 989-1052, 962-966, 1079-1136, 1261-2297, 1284-1185, 1299-586, 1300-349, 1303-396, 186-71, 655-572, 725-606, 1307-615				
Capacitor banks' location/ operation	Node	Modules	Type	Modules connected (reactive power injected [kVAr])		Node	Modules	Type	Modules connected (reactive power injected [kVAr])		Node	Modules	Type	Modules connected (reactive power injected [kVAr])	
				Level 1	Level 2				Level 1	Level 2				Level 1	Level 2
	1249	2	Switchable	2(1800)	0(0)	1249	2	Switchable	2(1786.83)	0(0.00)	1249	2	Switchable	2(1786.83)	0(0.00)
	1381	2	Fixed	2(1800)	2(1800)	1381	2	Fixed	2(1705.23)	2(1749.46)	1381	2	Fixed	2(1705.22)	2(1749.46)
	1459	1	Fixed	1(900)	1(900)	1459	1	Fixed	1(852.65)	1(874.88)	1459	1	Fixed	1(852.65)	1(874.87)
	1498	2	Switchable	2(1800)	1(900)	1931	2	Switchable	2(1657.56)	1(825.75)	1498	2	Switchable	2(1663.84)	1(830.42)
	1930	2	Switchable	2(1800)	1(900)	2102	1	Fixed	1(839.95)	1(851.36)	1930	2	Switchable	2(1664.66)	1(842.09)
	1931	2	Fixed	2(1800)	2(1800)	2259	2	Fixed	2(1775.46)	2(1766.73)	1931	2	Fixed	2(1661.17)	2(1684.08)
	2102	1	Fixed	1(900)	1(900)	2292	1	Fixed	1(840.91)	1(856.88)	2102	1	Fixed	1(836.98)	1(849.02)
	2259	2	Fixed	2(1800)	2(1800)	272	2	Switchable	2(1669.92)	1(832.76)	2259	2	Fixed	2(1775.45)	2(1766.73)
	2292	1	Fixed	1(900)	1(900)	317	2	Switchable	2(1634.85)	1(816.76)	2292	1	Fixed	1(840.91)	1(856.88)
	317	2	Switchable	2(1800)	1(900)	681	1	Fixed	1(832.36)	1(833.13)	317	2	Switchable	2(1634.85)	1(816.76)
	880	2	Switchable	2(1800)	1(900)	808	2	Switchable	2(1680.61)	1(839.72)	880	2	Switchable	2(1788.29)	1(886.64)
						880	2	Switchable	2(1788.29)	1(886.64)					

Table 9: Operational results for Cases A3 and A4

Results	Cases		
	B1	B2	Case B1 fixed in the complete model
Investment cost (USD)	60,000.00	63,800.00	60,000.00
Total losses cost (USD)	685,438.84	685,879.40	681,360.18
Total generation cost (USD)	150,091.39	151,064.00	151,064.06
Total cost (USD)	895,530.23	900,743.40	892,424.24
Node - Min. voltage (p.u.)			
Load level 1	1874 - 0.9508	1874-0.9500	1874 - 0.9487
Load level 2	1528 - 0.9522	1874-0.9511	1528 - 0.9517
Power losses (kW)			
Load level 1	1611.83	1637.19	1600.58
Load level 2	996.39	972.70	992.11
Losses cost reduction (%)	22.91	21.05	
CPU time (s)	4666	42893	–

For Case B1, after the reconfiguration and capacitor banks allocation, with a total investment cost of 60,000.00 USD (and their operation described in Table 8), the losses cost was reduced by 22.91%, to 685,438.84 USD, and all the voltage magnitudes are, in this case, within the limits of 0.95 p.u. and 1.05 p.u.

In Case B2, which considers voltage-dependent models, a similar reduction in the cost of losses in the system, of 19.92%, was obtained, when compared to Case B1. In this case, however, the topology of the system is different, and the investment in capacitor banks is larger (63,800.00 USD). It can be verified in the operation of the capacitor banks in Case B2 that the reactive power injections differ from the nominal values. Again, as for the 69-node system, the integer solution for Case B1 is infeasible when it is fixed in Case B2, due to the voltage magnitude violation at some nodes.

The computational times for the problem was 4666 s for Case B1 and 42893 s for Case B2, which is acceptable, since this is a large system and an operational planning problem. For all the tests performed for this system, it was verified that the conic constraint (5) was always active in the obtained solutions.

4.4 Dimension of the Proposed Model

The number of variables and constraints of the complete model for the reconfiguration of feeders and allocation of capacitor banks considering voltage-dependent models (M2) is presented in Table 10, where $|\cdot|$ represents the cardinality of the corresponding set, Ω_ℓ^* is the set of candidate nodes for the allocation of capacitor banks, and Ω_B^s is the set of branches directly connected to a substation node.

Table 10: Dimension of the proposed formulation

Variables	Continuous	$\|\Omega_L\|[2\|\Omega_N\| + 5\|\Omega_B\| + 2\|\Omega_s\| + \|\Omega_\ell^*\|(\|\Omega_C\| + 1) + 2\|\Omega_{DG}\|]$
	Integer	$\|\Omega_\ell^*\|$
	Binary	$2\|\Omega_B\| + \|\Omega_\ell^*\|(\|\Omega_C\|\|\Omega_L\| + 2)$
Constraints	Linear equality	$\|\Omega_B\| + 2\|\Omega_B^s\| + \|\Omega_\ell\| + \|\Omega_L\|(2\|\Omega_N\| + 2\|\Omega_B\| + \|\Omega_\ell^*\|)$
	Linear inequality	$\|\Omega_L\|[9\|\Omega_B\| + 2\|\Omega_\ell\| + 2\|\Omega_{DG}\| + \|\Omega_\ell^*\|(5\|\Omega_C\| + 1)] + 1$
	Quadratic	$(\|\Omega_s\| + \|\Omega_{DG}\|)\|\Omega_L\|$
	Conic	$\|\Omega_B\|\|\Omega_L\|$

The main difficulty of the model presented in this paper is related to the presence of discrete (binary and integer) variables. Table 10 shows that the number of integer variables in the problem is equal to $|\Omega_\ell^*|$ while the number of binary variables is $2|\Omega_B| + |\Omega_\ell^*|(|\Omega_C||\Omega_L| + 2)$. Therefore, by reducing the number of candidate nodes for the installation of capacitor banks, the number of load levels, or the number of capacitor modules that can be installed at a node, the number of discrete variables is also reduced. As presented in the previous section, it was possible to find a solution for the 2313-node real system by performing the proposed strategy for defining candidate nodes for the installation of capacitor banks.

5. Discussion

In the literature, most of the works use heuristic and metaheuristic strategies for solving the distribution feeders' reconfiguration problem and the capacitor bank size and allocation problem, either considering only one problem or both problems simultaneously. Although heuristic-based strategies achieve good-quality solutions, these approaches cannot ensure convergence to optimality. In this work, a mixed-integer second-order cone programming formulation, which guarantees convergence to the optimal solution, is proposed. Moreover, the results presented in Section 4, for the 69-node and the real 2313-node systems, demonstrate the effectiveness and the scalability of the proposed approach. On the other hand, the proposed strategy for the reduction of candidate nodes for capacitor banks allocation validates its effectiveness by obtaining a set of candidate nodes that includes all nodes where capacitor banks are installed when solving the complete model without reducing the search space, as shown in Section 4.2. The results presented in Section 4.1 show the importance of considering voltage-dependent models for the loads and capacitors banks. Neglecting voltage-dependent formulations could lead to economic losses due to unnecessary or wrong investments or, even worse, compromising the system's operation. The importance of performing the simultaneous reconfiguration of feeders and allocation of capacitor banks is evidenced when these problems are solved sequentially—it is not possible to obtain a feasible solution by solving either the reconfiguration and then the allocation of capacitor banks or the allocation of capacitor banks and then the reconfiguration problem.

6. Conclusion

In this paper, a model for the simultaneous reconfiguration of feeders and allocation of capacitor banks in radial distribution systems was presented. The mathematical model considers voltage dependence for capacitor banks and load models. The optimization problem was addressed as a mixed-integer second-order cone programming model that is convex and, therefore, guarantees convergence to optimality by using commercial solvers. A strategy to reduce the combinatorial search space of the problem by defining candidate nodes for the installation of capacitor banks was presented. The proposed approach has been tested in a modified 69-node radial system for several study cases, combining different load and capacitor models, and in a 2313-node real distribution system, to demonstrate the scalability of the proposal. It is concluded that the load and capacitor modeling have a significant impact on the investment plan. As presented in this work, not considering the voltage dependence model for loads and capacitor banks can lead to infeasible solutions when these solutions are evaluated in the complete model

with both voltage-dependent loads and capacitor banks models. According to the results, the simultaneous reconfiguration of feeders and allocation of the capacitor banks can improve the voltage regulation and minimize the power losses by load relocation and control of the reactive power flow. It was also verified that trying to solve the reconfiguration problem and then the problem of the allocation of capacitor banks, sequentially, may lead to infeasible solutions.

7. Acknowledgment

This work was supported by the Coordination for the Improvement of Higher Education Personnel (CAPES) – Finance Code 001, the Brazilian National Council for Scientific and Technological Development (CNPq), and the São Paulo Research Foundation (FAPESP), under grants 2014/23741-9 and 2015/21972-6.

References

[1] Gönen T. Electric power distribution system engineering. 2nd ed. Boca Raton: CRC Press; 2008.

[2] Georgilakis PS, Hatziargyriou ND. A review of power distribution planning in the modern power systems era: models, methods and future research. Electr Power Syst Res 2015;121:89–100. doi:10.1016/j.epsr.2014.12.010.

[3] Yamangil E, Bent R, Backhaus S. Designing resilient electrical distribution grids. ArXiv Prepr 2014.

[4] Yuan W, Wang J, Qiu F, Chen C, Kang C, Zeng B. Robust optimization-based resilient distribution network planning against natural disasters. IEEE Trans Smart Grid 2016;7:2817–26. doi:10.1109/TSG.2015.2513048.

[5] Grainger JJ, Lee SH. Capacity release by shunt capacitor placement on distribution feeders: a new voltage-dependent model. IEEE Trans Power Appar Syst 1982;PAS-101:1236–44. doi:10.1109/TPAS.1982.317385.

[6] Baran ME, Wu FF. Optimal capacitor placement on radial distribution systems. IEEE Trans Power Deliv 1989;4:725–34. doi:10.1109/61.19265.

[7] Gallego RA, Monticelli AJ, Romero R. Optimal capacitor placement in radial distribution networks. IEEE Trans Power Syst 2001;16:630–7. doi:10.1109/59.962407.

[8] Das D. Optimal placement of capacitors in radial distribution system using a Fuzzy-GA method. Int J Electr Power Energy Syst 2008;30:361–7. doi:10.1016/j.ijepes.2007.08.004.

[9] El-Fergany AA, Abdelaziz AY. Efficient heuristic-based approach for multi-objective capacitor allocation in radial distribution networks. IET Gener Transm Distrib 2014;8:70–80. doi:10.1049/iet-gtd.2013.0213.

[10] Vuletić J, Todorovski M. Optimal capacitor placement in distorted distribution networks with different load models using penalty free genetic algorithm. Int J Electr Power Energy Syst 2016;78:174–82. doi:10.1016/j.ijepes.2015.11.065.

[11] Jabr RA. Optimal placement of capacitors in a radial network using conic and mixed integer linear programming. Electr Power Syst Res 2008;78:941–8. doi:10.1016/j.epsr.2007.07.002.

[12] Baran ME, Wu FF. Network reconfiguration in distribution systems for loss reduction and load balancing. IEEE Trans Power Deliv 1989;4:1401–7. doi:10.1109/61.25627.

[13] Shirmohammadi D, Hong HW. Reconfiguration of electric distribution networks for resistive line losses reduction. IEEE Trans Power Deliv 1989;4:1492–8. doi:10.1109/61.25637.

[14] Jeon Y-J, Kim J-C, Kim J-O, Shin J-R, Lee KY. An efficient simulated annealing algorithm for network

reconfiguration in large-scale distribution systems. IEEE Trans Power Deliv 2002;17:1070–8. doi:10.1109/TPWRD.2002.803823.

[15] Abdelaziz AY, Mohamed FM, Mekhamer SF, Badr MAL. Distribution system reconfiguration using a modified tabu search algorithm. Electr Power Syst Res 2010;80:943–53. doi:10.1016/j.epsr.2010.01.001.

[16] Mendoza J, López R, Morales D, López E, Dessante P, Moraga R. Minimal loss reconfiguration using genetic algorithms with restricted population and addressed operators: real application. IEEE Trans Power Syst 2006;21:948–54. doi:10.1109/TPWRS.2006.873124.

[17] Carreno EM, Romero R, Padilha-Feltrin A. An efficient codification to solve distribution network reconfiguration for loss reduction problem. IEEE Trans Power Syst 2008;23:1542–51. doi:10.1109/TPWRS.2008.2002178.

[18] Torres J, Guardado JL, Rivas-Dávalos F, Maximov S, Melgoza E. A genetic algorithm based on the edge window decoder technique to optimize power distribution systems reconfiguration. Int J Electr Power Energy Syst 2013;45:28–34. doi:10.1016/j.ijepes.2012.08.075.

[19] Barbosa CHN de R, Mendes MHS, de Vasconcelos JA. Robust feeder reconfiguration in radial distribution networks. Int J Electr Power Energy Syst 2014;54:619–30. doi:10.1016/j.ijepes.2013.08.015.

[20] Naveen S, Kumar KS, Rajalakshmi K. Distribution system reconfiguration for loss minimization using modified bacterial foraging optimization algorithm. Int J Electr Power Energy Syst 2015;69:90–7. doi:10.1016/j.ijepes.2014.12.090.

[21] Jabr RA, Singh R, Pal BC. Minimum loss network reconfiguration using mixed-integer convex programming. IEEE Trans Power Syst 2012;27:1106–15. doi:10.1109/TPWRS.2011.2180406.

[22] Franco JF, Rider MJ, Lavorato M, Romero R. A mixed-integer LP model for the reconfiguration of radial electric distribution systems considering distributed generation. Electr Power Syst Res 2013;97:51–60. doi:10.1016/j.epsr.2012.12.005.

[23] Singh D, Misra RK. Load type impact on distribution system reconfiguration. Int J Electr Power Energy Syst 2012;42:583–92. doi:10.1016/j.ijepes.2012.04.032.

[24] Rong Z, Xiyuan P, Jinliang H, Xinfu S. Reconfiguration and capacitor placement for loss reduction of distribution system. 2002 IEEE Reg. 10 Conf. Comput. Commun. Control Power Eng. TENCOM '02., vol. 3, Beijing: 2002, p. 1945–9. doi:10.1109/TENCON.2002.1182719.

[25] Venkatesh B, Ranjan R. Fuzzy EP algorithm and dynamic data structure for optimal capacitor allocation in radial distribution systems. IEE Proc - Gener Transm Distrib 2006;153:80–8. doi:10.1049/ip-gtd:20050054.

[26] Yang L, Guo Z. Comprehensive optimization for energy loss reduction in distribution networks. 2008 IEEE Power Energy Soc. Gen. Meet. - Convers. Deliv. Electr. Energy 21st Century, Pittsburgh: 2008, p. 1–8. doi:10.1109/PES.2008.4595980.

[27] Chang C-F. Reconfiguration and capacitor placement for loss reduction of distribution systems by ant colony search algorithm. IEEE Trans Power Syst 2008;23:1747–55. doi:10.1109/TPWRS.2008.2002169.

[28] Guimarães MAN, Castro CA, Romero R. Distribution systems operation optimisation through reconfiguration and capacitor allocation by a dedicated genetic algorithm. IET Gener Transm Distrib 2010;4:1213–22. doi:10.1049/iet-gtd.2010.0020.

[29] de Oliveira LW, Carneiro S, de Oliveira EJ, Pereira JLR, Silva IC, Costa JS. Optimal reconfiguration and capacitor allocation in radial distribution systems for energy losses minimization. Int J Electr Power Energy Syst 2010;32:840–8. doi:10.1016/j.ijepes.2010.01.030.

[30] Farahani V, Vahidi B, Abyaneh HA. Reconfiguration and capacitor placement simultaneously for energy loss reduction based on an improved reconfiguration method. IEEE Trans Power Syst 2012;27:587–95. doi:10.1109/TPWRS.2011.2167688.

[31] Esmaeilian HR, Fadaeinedjad R. Distribution system efficiency improvement using network reconfiguration and capacitor allocation. Int J Electr Power Energy Syst 2015;64:457–68. doi:10.1016/j.ijepes.2014.06.051.

[32] Sayadi F, Esmaeili S, Keynia F. Feeder reconfiguration and capacitor allocation in the presence of non-linear loads using new P-PSO algorithm. IET Gener Transm Distrib 2016;10:2316–26. doi:10.1049/iet-gtd.2015.0936.

[33] Sultana S, Roy PK. Oppositional krill herd algorithm for optimal location of capacitor with reconfiguration in radial distribution system. Int J Electr Power Energy Syst 2016;74:78–90.

doi:10.1016/j.ijepes.2015.07.008.

[34] Sedighizadeh M, Esmaili M, Eisapour-Moarref A. Hybrid symbiotic organisms search for optimal fuzzified joint reconfiguration and capacitor placement in electric distribution systems. Ina Lett 2017;2:107–21. doi:10.1007/s41403-017-0029-5.

[35] Evangelopoulos VA, Georgilakis PS, Hatziargyriou ND. Optimal operation of smart distribution networks: a review of models, methods and future research. Electr Power Syst Res 2016;140:95–106. doi:10.1016/j.epsr.2016.06.035.

[36] Jiang D, Baidick R. Optimal electric distribution system switch reconfiguration and capacitor control. IEEE Trans Power Syst 1996;11:890–7. doi:10.1109/59.496171.

[37] Ameli A, Ahmadifar A, Shariatkhah M-H, Vakilian M, Haghifam M-R. A dynamic method for feeder reconfiguration and capacitor switching in smart distribution systems. Int J Electr Power Energy Syst 2017;85:200–11. doi:10.1016/j.ijepes.2016.09.008.

[38] Gutiérrez-Alcaraz G, Tovar-Hernández JH. Two-stage heuristic methodology for optimal reconfiguration and Volt/VAr control in the operation of electrical distribution systems. IET Gener Transm Distrib 2017;11:3946–54. doi:10.1049/iet-gtd.2016.1870.

[39] Ding T, Liu S, Yuan W, Bie Z, Zeng B. A two-stage robust reactive power optimization considering uncertain wind power integration in active distribution networks. IEEE Trans Sustain Energy 2016;7:301–11. doi:10.1109/TSTE.2015.2494587.

[40] Glover F, Kochenberger GA. Handbook of metaheuristics. 1st ed. Dordrecht: Kluwer Academic Publishers; 2003.

[41] Hajagos LM, Danai B. Laboratory measurements and models of modern loads and their effect on voltage stability studies. IEEE Trans Power Syst 1998;13:584–92. doi:10.1109/59.667386.

[42] Farivar M, Low SH. Branch flow model: relaxations and convexification—part I. IEEE Trans Power Syst 2013;28:2554–64. doi:10.1109/TPWRS.2013.2255317.

[43] Franco JF, Rider MJ, Romero R. A mixed-integer quadratically-constrained programming model for the distribution system expansion planning. Int J Electr Power Energy Syst 2014;62:265–72. doi:10.1016/j.ijepes.2014.04.048.

[44] Fourer R, Gay DM, Kernighan BW. AMPL: a modeling language for mathematical programming. 2nd ed. Duxbury: Thomson; 2003.

[45] IBM. CPLEX optimization studio v12.8 2018:594. http://www-01.ibm.com/support/docview.wss?uid=swg27050618 (accessed June 23, 2018).

[46] Chiang H-D, Jean-Jumeau R. Optimal network reconfigurations in distribution systems: part 2: Solution algorithms and numerical results. IEEE Trans Power Deliv 1990;5:1568–74. doi:10.1109/61.58002.

[47] LaPSEE Power System Test Cases Repository 2018. http://www.feis.unesp.br/#!/lapsee (accessed June 25, 2018).